MTTM

Megha-Tropiques Technical Memorandum

TAPEER-BRAIN PRODUCT
Algorithm Theoretical Basis Document
Level 4

Philippe Chambon, Rémy Roca, Isabelle Jobard, Jérémie Aublanc

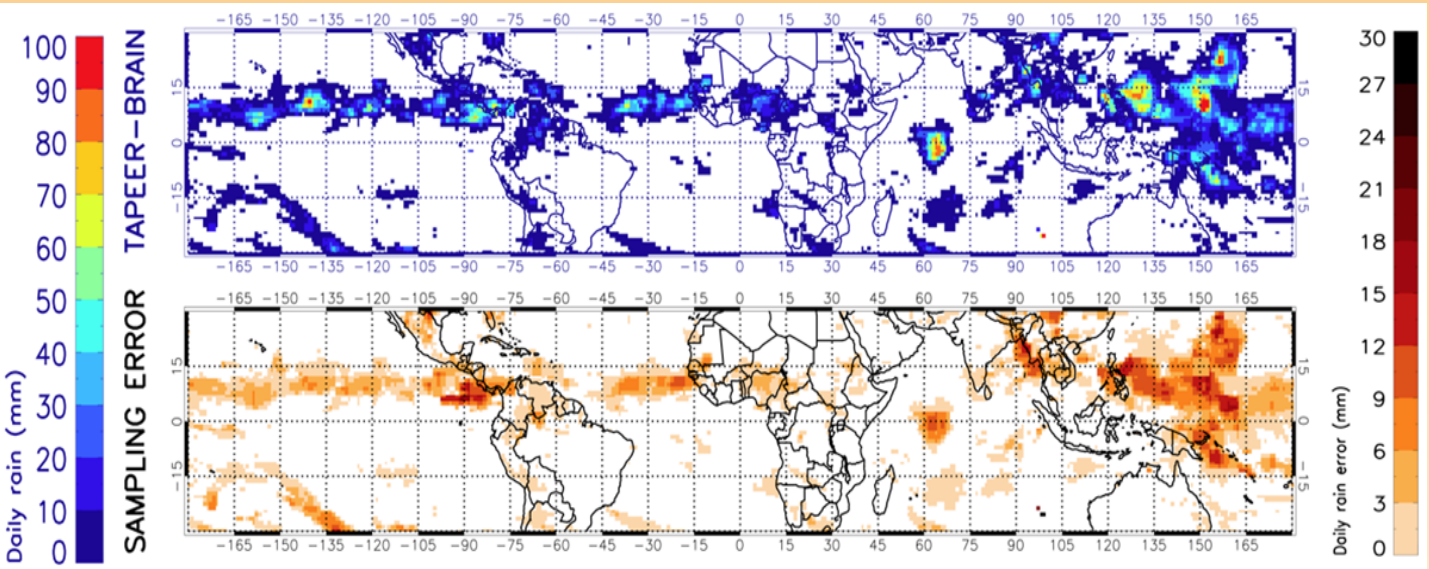

February 2012

04

TAPEER-BRAIN Product

Algorithm Theoretical Basis Document

Level 4

Philippe Chambon, Rémy Roca, Isabelle Jobard, Jérémie Aublanc

Laboratoire de Météorologie Dynamique (LMD/IPSL)

February 2012

1. Introduction

TAPEER-BRAIN is a combined Microwave-Infrared accumulated precipitation estimation product implemented as a Megha-Tropiques Level 4 product. TAPEER stands for Tropical Amount of Precipitation with an Estimate of ERrors. It provides precipitation estimations and associated errors at the one-degree/one-day accumulated scale. TAPEER-BRAIN is based on the BRAIN algorithm (Viltard et al., 2006, MT Level 2 MW-derived instantaneous rain estimation product) and the TAPEER algorithm.

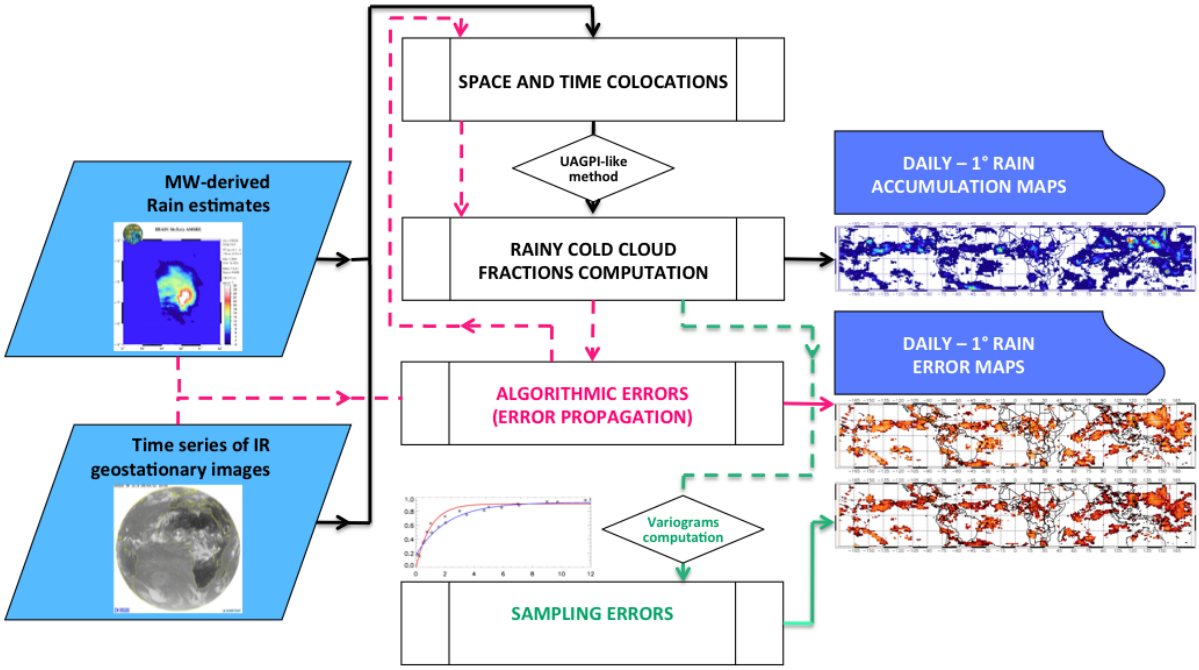

Figure 1 : General diagram

The TAPEER algorithm relies on two separate algorithms to provide both the Tropical Amount of Precipitation and the Estimate of ERrors. Figure 1 summarizes the functioning of the algorithm with black arrows standing for the Tropical Amount of Precipitation computations, green arrows and pink arrows standing for the Estimate of ERrors computations.

2. Algorithms

2.1 Tropical Amount of Precipitation

The Tropical Amount of Precipitation is estimated with a combination of MW-derived rain estimations and time series of geostationary Thermal Infrared data (TIR). Figure 2 illustrates the need of MW and TIR data combination to estimate rainfall at the accumulated scale: a rainy event occurred on the 8th of September 2006 over Niamey and led to one of the most important daily rain accumulation (18.5 mm +/-2.1 mm) in the rain gauge records for the 2006 monsoon season. This rainy event has not been observed by any MW imager of a constellation of four low earth-orbiting satellites, but was monitored by the multispectral imager SEVIRI onboard the geostationary satellite Meteosat Second Generation (top line). IR monitoring provides information only statistically related to rainfall accumulated on long periods and averaged over large areas. Thus MW-derived estimations are jointly used with IR data to provide an Amount of Precipitation. The method of combination of TIR data and MW-derived rain rates selected for TAPEER relies on the Universally Adjusted GOES Precipitation Index (UAGPI) technique (Xu et al., 1999) which aims to estimate rain accumulation through cold cloud fraction calculations.

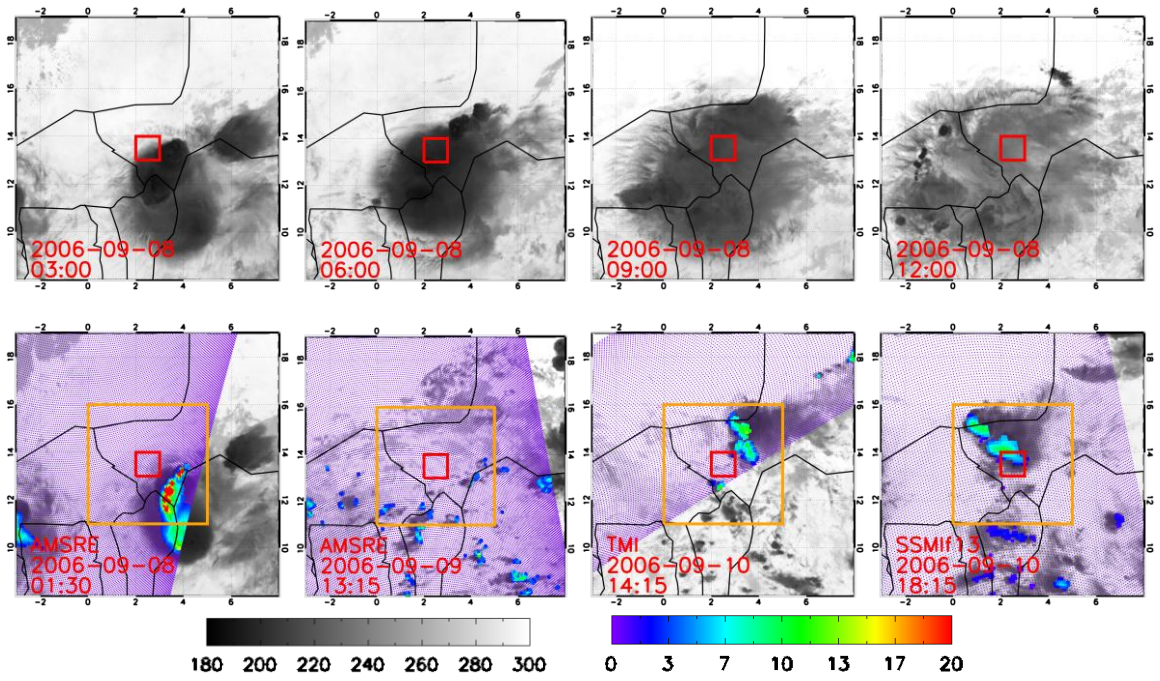

Figure 2: Time series (first line) of Infrared Brightness temperatures (in Kelvin, grey colorbar) images for the 8th of September 2006 over the region of Niamey, Niger (the red and orange squares correspond to the 1° and 5° areas close to the rain gauge network of Niamey). Time series (secondline) of Infrared Brightness temperatures images during the period ±2-days off the 8th of September 2006, selected when the BRAIN algorithm, from a constellation of passive MW imagers, provides rain estimations (in $mm.h^{-1}$, rainbow colorbar)

The UAGPI relates accumulated rainfall, in a given area A over a period T, $< R >_{A;T}$ to the rainy cloud fraction Fc in this space-time-volume, working on the assumption that for large enough areas and accumulation times, rainfall rates in this volume tend towards a local mean value R_{COND} that may be determined through the use of available local microwave satellite precipitation data. For instance, Figure 2 (bottom line) illustrates the available local microwave satellite precipitation data for the one-degree area of Niamey on the 8th of September 2006, in a volume of 5° x 5° x 5-day surrounding the 1°/1-day volume. With an estimate of the rainy cloud fraction Fc and the local mean rain rate value R_{COND}, the following equation is used to compute the Tropical Amount of Precipitation:

$$< R >_{A;T} = F_C \, . \, R_{COND} \, . \, T \qquad \textbf{(1)}$$

The rainy cloud fraction Fc, for a period T (24 h) and a given area A (1°x 1°), is estimated with TIR data under the following assumption: TIR samples colder (resp. warmer) than a given threshold $T_{threshold}$ are assumed to be rainy (resp. non-rainy). From the GATE experiment in Tropical Atlantic, it was shown that a 235 K threshold was a good compromise when estimating monthly and 2.5° x 2.5° rainy cloud fractions (Arkin, 1979).

Numerous studies have demonstrated that $T_{threshold}$ can be adapted to local meteorological conditions for a more accurate estimation of the rainy cloud fraction, at scales shorter than a month and for areas smaller than 2.5°x 2.5°(Adler et al., 1993; Xu et al., 1999; Huffman et al., 2001; Todd et al., 2001; Kidd et al., 2003).

One method to adapt $T_{threshold}$ to local meteorological conditions is to work with local distributions of MW-derived rain estimations, collocated with TIR data, and perform a histogram matching. Figure 3 shows an example of the procedure: local distributions of Infrared and Rainfall data are collected in a 5° x 5° x 5-day volume, surrounding a 1°/1-day volume in which **F**C needs to be estimated. These distributions are cumulated to derive cumulated distribution functions. $T_{threshold}$ is then set so that the fraction of collocated TIR data warmer than this threshold is equal to the fraction of non-rainy collocated Rain Rates. In the example of Figure 3, 75% of the MW-derived rain samples are non-rainy samples: $T_{threshold}$ is then set to approximately 240 K. The second parameter R_{COND} is set to the mean rainy value of this distribution for keeping the rain volume estimated in the MW-derived rain rate local distribution.

The cloud top temperature/rainfall relationship is likely to vary over a wide range of scales, from inter-annual to sub-daily scales depending on the physical properties of the environment of rainy events like the tropical wave dynamics (Machado et al., 1993), the relative humidity available in the boundary layer (Roca et al., 2005), soil moisture (Taylor et al., 2010), local solar time (Laing et al., 2008).

This simple histogram matching method converges toward values of $T_{threshold}$ and R_{COND} depending on the volume of data used for their computation. This volume of data, called training volume in the following, has two characteristics: the size of the geographical domain and the duration of the period considered for the training of a 1°/1-day rain estimation.

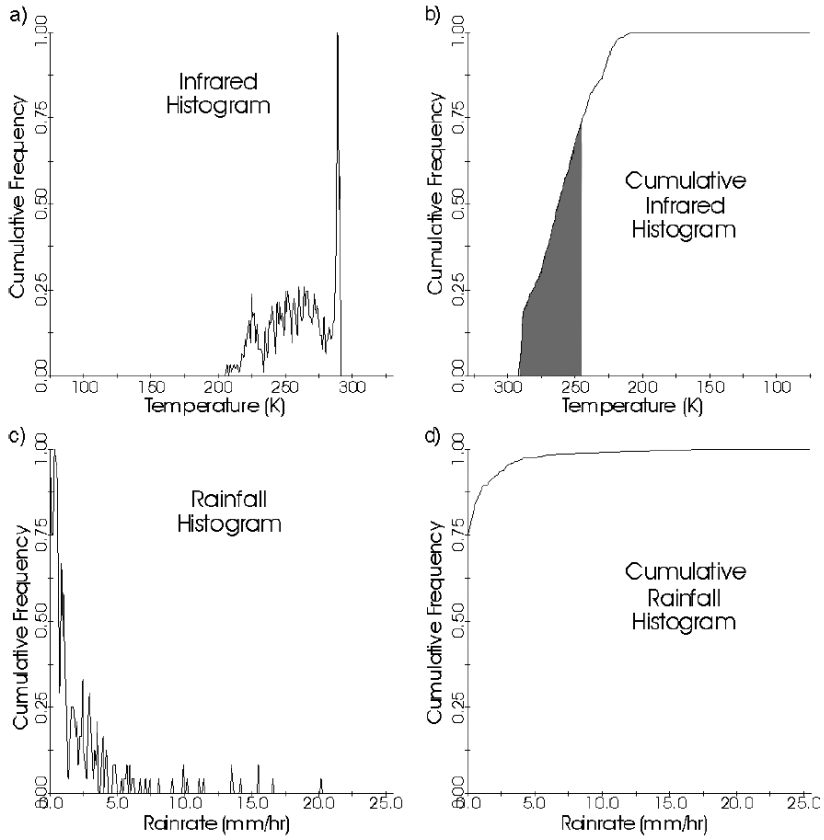

Figure 3: Distributions of Infrared pixels (top left) and MW-derived rain rates (bottom left). Cumulated distributions of IR pixels (top right) and MW-derived rain rates (bottom right) for a 5˚x 5˚x 5-days volume (Kidd et al., 2003)

The two parameters $T_{threshold}$ and R_{COND} are computed for all the 1°x1°x1-day volumes of the whole Tropics and for a given period. The local volumes of collocated data are chosen to overlap each other with a moving window of 5° x 5° x 5-day to avoid large discontinuities in the ($T_{threshold}$, R_{COND}) fields. For each day of the period, maps of parameters ($T_{threshold}$, R_{COND}) are then created. Figure 4 shows an example of two maps of $T_{threshold}$ and R_{COND} used to compute a rain accumulation map. One can see that in the Tropical Atlantic ocean, the two parameters are close to 235 K and 3 $mm.h^{-1}$ as found during the GATE experiment, but exhibit a large variability over the whole Tropical belt. In particular, large regions like the Sahelian band or the Northern part of Bay of Bengal present very cold $T_{threshold}$ under 200 K to exclude raining from non-raining clouds. This variability demonstrates the geographical dependence of the cloud top temperature/rainfall relationship and confirms the need of their local computation.

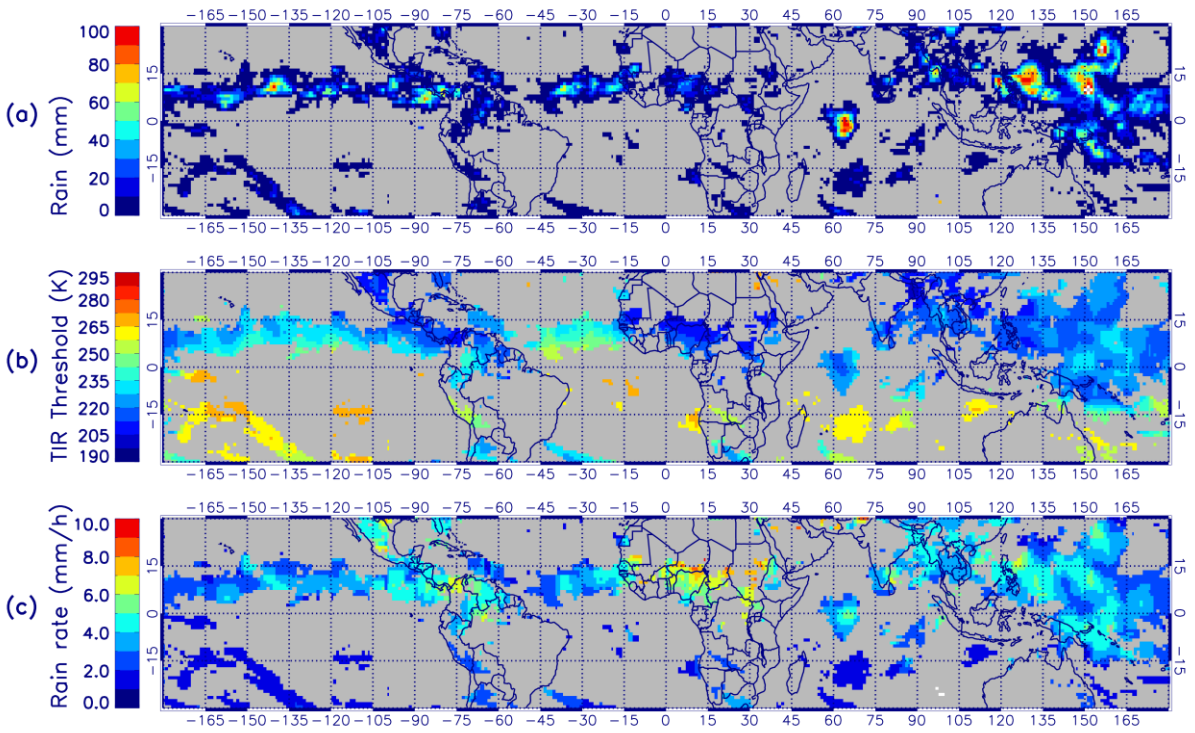

Figure 4: $T_{threshold}$ (middle) and R_{COND} (bottom) used to compute a TAPEER 1°/1-day precipitation map (top)

The size of the geographical domain and the duration of the period of the training volume are two parameters of the TAPEER algorithm. They are closely related to a third degree of freedom: the configuration of the constellation of Passive MW Observing Systems. In Chambon (2011), we show a sensitivity study of these three degrees of freedom on the Tropical Amount of Precipitation as well as on the Estimate of ERrors. Depending on the number of Passive MW Observing Systems available, the training volume can be selected in order to compute 1°/1-day best estimates.

In order to compute the rainy cloud fraction FC for each 1° x 1° x 1-day volume, time series of TIR geostationary images are segmented: TB warmer than the local $T_{threshold}$ are set to "0" (non rainy) samples and TB colder than the local $T_{threshold}$, are set to "1" (rainy) samples. These Rain/No-Rain maps are then aggregated and averaged to compute local FC. $< R >_{A;T}$ is then derived using Equation 1. Another technical solution, which was chosen in the present implementation of the TAPEER algorithm, is to assign 0 $mm.h^{-1}$ to TB warmer than the local $T_{threshold}$, and R_{COND} $mm.h^{-1}$ to TB colder than the local $T_{threshold}$. The rain rates maps are then averaged at the 1° x 1° x 1-day. In this case, the rain rates maps may be seen as instantaneous rain samples at the high resolution of geostationary TIR data. These rain samples are contaminated by very large random errors due to the very loose physical/statistical relationship on which their computation is based. These random errors average out when the rain rates maps are aggregated at the accumulated scale.

2.2 Estimate of Errors

The error budget of satellite rainfall estimations is composed of a sum of three terms, under the assumption that error sources are uncorrelated. These different terms are added to compute the Estimate of ERrors in the TAPEER algorithm:

$$S^2 = S^2_{Sampling} + S^2_{Algorithm} + S^2_{Calibration} \qquad (2)$$

Both $S^2_{Algorithm}$ and $S^2_{Calibration}$ terms are the consequence of the errors on the two data sources used in TAPEER: MW-derived rain estimations and TIR brightness temperature data. Errors on these two data sources can be large, especially for the MW-derived rain estimations, and possibly be magnified in the area-integrated rain accumulations. To account for these error sources in the error computed in the TAPEER algorithm, a forward error propagation technique was developed (Chambon et al., 2011). This technique leads to an estimation of $S^2_{Algorithm}$ and $S^2_{Calibration}$ for realistic magnitude of errors on MW derived rainfall estimation algorithms and on TIR brightness temperature data.

The $S^2_{Sampling}$ term represents the error related to the discrete nature of measurements in space and time, used to estimate an area-integrated rain accumulation. An error model involving variograms computation is used to estimate this first term (Roca et al., 2010). This model consists in the computation of the variance of estimation of a mean, given σ^2 the variance of the samples and $N_{Independent}$ the number of independent samples composing the mean rainfall accumulation:

$$S^2_{Sampling} = \frac{\sigma^2}{N_{Independent}} \qquad (3)$$

For this model, a local estimate of $N_{Independent}$ is required. To this end, local space and time variograms, $\gamma(\Delta x, t_0)$ and $\gamma(\vec{x}_0, \Delta t)$, are computed to extract $N_{Independent}$ from the samples constituting $< R >_{A;T}$. These samples are the "0" (non rainy) samples and "1" (rainy) samples or the 0 $mm.h^{-1}$ samples and R_{COND} $mm.h^{-1}$ samples discussed above. In order to avoid the contamination of variograms by the large random errors in the rain rate maps, variograms are computed over the rain/no-rain fields or Indicator fields (noted IF fields below) (Barancourt et al., 1992).

For a slot t_0 of the IF time series, the space variogram $\gamma(\Delta x, t_0)$ can be expressed with the Equation 4 where Δx is the lag space between two samples, $n(\Delta x)$ is the number of pairs of samples distant of Δx, and $\sigma^2_{space}(t_0)$ the variance of the IF field over the area and at the slot t_0 where the space variogram is computed.

$$\gamma(\Delta x = \left\| \vec{x}_1 - \vec{x}_0 \right\|, t_0) = \frac{\frac{1}{n(\Delta x)} \sum_{i=0}^{n(\Delta x)} [IF(\vec{x}_1, t) - IF(\vec{x}_0, t)]^2}{\sigma^2_{space}(t_0)} \qquad (4)$$

For a location $\vec{x}_0$ of the IF fields, the time variogram $\gamma(\vec{x}_0, \Delta t)$ can be expressed with the Equation 5 where Δt is the lag time between two samples, $m(\Delta t)$ is the number of pairs of

samples distant of Δt and $\sigma^2_{time}(\vec{x}_0)$ the variance of the IF fields over the period and the location $\vec{x}_0$ where the time variogram is computed.

$$\gamma(\vec{x}_0, |t_1 - t_0|) = \frac{\frac{1}{m(\Delta t)} \sum_{i=0}^{m(\Delta t)} [IF(\vec{x}_0, t_1) - IF(\vec{x}_0, t_0)]^2}{\sigma^2_{time}(\vec{x}_0)} \qquad (5)$$

Figure 5 shows a part of the time series of IF fields used to compute Figure 6 of Chambon et al. (2011). Over each image of 5° x 5°, a space variogram can be computed: $\gamma(\Delta x, t_0)$ for the slot t_0, $\gamma(\Delta x, t_1)$ for the slot t_1, etc. For each pixel, a time series over a given period can be extracted (red lines of Figure 5) ; a time variogram can be computed : $\gamma(\vec{x}_0, \Delta t)$ for the pixel at position $\vec{x}_0$, $\gamma(\vec{x}_1, \Delta t)$ for the pixel at position $\vec{x}_1$.

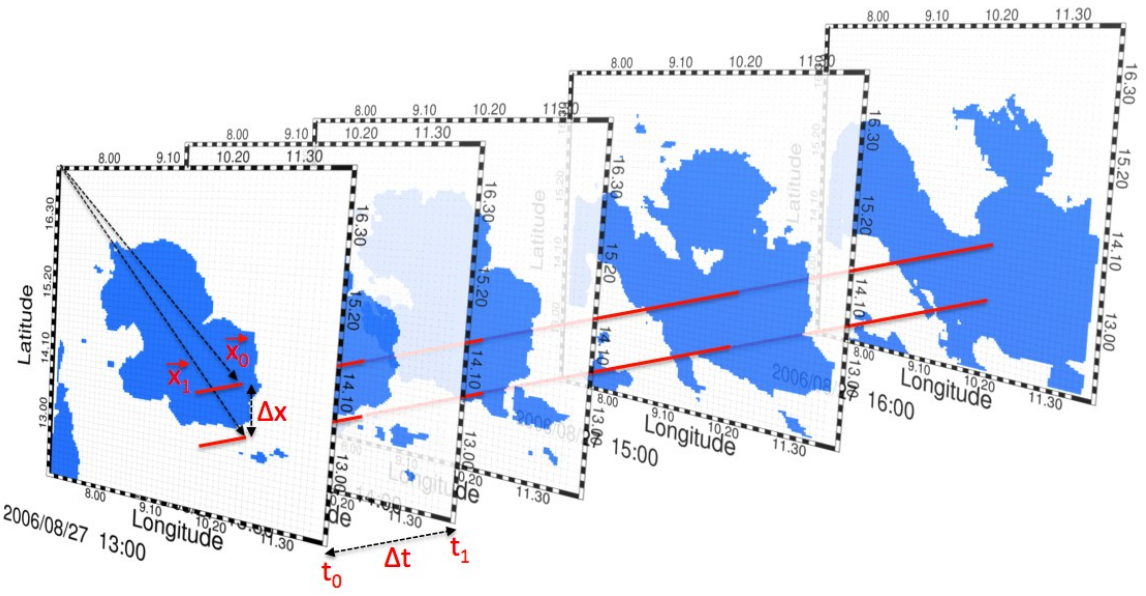

Figure 5: Time series of TAPEER-BRAIN Indicator fields for the region [7°E - 12°E; 12°N - 17°N]. , The two red lines, positioned at $\vec{x}_0$ and $\vec{x}_1$ show the time series over which two time variograms $\gamma(\vec{x}_0, \Delta t)$ and $\gamma(\vec{x}_1, \Delta t)$ can be computed.

Deriving an estimate of $N_{Independent}$ in a 1° x 1° x 1-day volume requires the averaging of variograms over the volume. Indeed, where a single variogram reflects the autocorrelation of only a fraction of the samples composing the mean rainfall accumulation, averaged space and time variograms $\Gamma_{A,T}(\Delta x)$ and $\Gamma_{A,T}(\Delta t)$ reflect the ensemble autocorrelation:

$$\Gamma_{A,T}(\Delta x) = \frac{1}{N_{t_0 \in T}} \sum_{t_0 \in T} \gamma(\Delta x, t_0) \qquad (6)$$

$$\Gamma_{A,T}(\Delta t) = \frac{1}{M_{\vec{x}_0 \in A}} \sum_{\vec{x}_0 \in A} \gamma(\vec{x}_0, \Delta t) \qquad (7)$$

Figure 3 of Roca et al. (2010) shows $\Gamma_{A,T}(\Delta x)$ and $\Gamma_{A,T}(\Delta t)$ for three different satellite products and the modeling of them by an exponential function. In the TAPEER algorithm, $\Gamma_{A,T}(\Delta x)$ and $\Gamma_{A,T}(\Delta t)$ are also modeled by exponential functions and the derived space and time e-folding distances d and τ are used to compute $N_{Independent}$ using the following equation:

$$N_{independent} = \frac{A.T}{d^2.\tau} \qquad (8)$$

In terms of practical considerations, using a domain larger than 1° x 1° x 1-day to average variogram functions $\Gamma_{A,T}(\Delta x)$ and $\Gamma_{A,T}(\Delta t)$ leads to more robust variograms. A compromise between averaging variograms for robustness and detecting the variability of d and τ parameters was found to be an averaging volume of 5° x 5° x 10-days. Variogram calculations are time consuming, so the following assumptions are used to limit computation cost:

- A regular space grid is assumed in 5° x 5° domains of geostationary TIR data, variations in inter-pixel distance are only taken into account from a 5° x 5° domain to another 5° x 5°.
- The smaller time resolution of geostationary TIR data is 30 minutes.
- An exponential model is assumed for all variograms.
- 5° x 5° x 10-days domains do not overlap each other, d and τ are considered to be constant inside such a volume.

References

Adler, R., Negri, A., Keehn, P., and Hakkarinen, I. (1993). Estimation of monthly rainfall over Japan and surrounding waters from a combination of low-orbit microwave and geosynchronous IR data. J. Appl. Meteorol., 32(2), 335–356.

Arkin, P. (1979). The relationship between fractional coverage of high cloud and rainfall accumulations during gate over the b-scale array. Mon. Weather Rev., 107, 1382–1387.

Barancourt, C., Creutin, J., and Rivoirard, J. (1992). A method for delineating and estimating rainfall fields. Water Resour. Res., 28(4), 1133–1144.

Chambon P. 2011. 'Contribution à l'estimation des précipitations Tropicales: préparation aux missions Megha-Tropiques et Global Precipitation Measurement', PhD Thesis, 199pp. Université Paris-Est.

Chambon, P., Jobard, I., Roca, R., and Viltard, N. (2012). An investigation of the error budget of tropical rainfall accumulation derived from merged passive microwave and infrared satellite measurements. Quart. J. Roy. Meteorol. Soc. 138:000-000. DOI:10.1002/qj. 1907

Huffman, G., Adler, R., Morrissey, M., Bolvin, D., Curtis, S., Joyce, R., McGavock, B., and Susskind, J. (2001). Global precipitation at one-degree daily resolution from multisatellite observations. J. Hydrometeor., 2(1), 36–50.

Kidd, C., Kniveton, D., Todd, M., and Bellerby, T. (2003). Satellite rainfall estimation using combined passive microwave and infrared algorithms. J. Hydrometeor., 4(6), 1088–1104.

Laing, A., Carbone, R., Levizzani, V., and Tuttle, J. (2008). The propagation and diurnal cycles of deep convection in northern tropical africa. Quart. J. Roy. Meteorol. Soc., 134(630), 93–109.

Machado, L., Duvel, J., and Desbois, M. (1993). Diurnal variations and modulation by easterly waves of the size distributions of convective cloud clusters over west africa and the atlantic ocean. Mon. Weather Rev., 121, 37–49.

Roca, R., Lafore, J.-P., Piriou, C., and Redelsperger, J.-L. (2005). Extratropical dry-air intrusions into the West African monsoon midtroposphere: An important factor for the convective activity over the Sahel. J. Atmos. Sci., 62(2), 390–407.

Roca, R., Chambon, P., Jobard, I., Kirstetter, P.-E., Gosset, M., and Bergès, J.-C. (2010). Comparing satellite and surface rainfall products over West Africa at meteorologically relevant scales during the AMMA campaign using error estimates. J. Appl. Meteorol. and Climatol., 49(4), 715–731.

Taylor, C., Harris, P., and Parker, D. (2010). Impact of soil moisture on the development of a Sahelian mesoscale convective system : A case-study from the AMMA special observing period. Quart. J. Roy. Meteorol. Soc. 136(51), 456-470.

Todd, M., Kidd, C., Kniveton, D., and Bellerby, T. (2001). A combined satellite infrared and passive microwave technique for estimation of small-scale rainfall. J. Atmos. Ocean. Technol., 18(5), 742–755.

Viltard, N., Burlaud, C., and Kummerow, C. (2006). Rain retrieval from TMI brightness temperature measurements using a TRMM pr–based database. J. Appl. Meteorol. and Climatol., 45, 455–466.

Xu L, Gao X, Sorooshian S, Arkin PA, Imam B. (1999). A microwave infrared threshold technique to improve the GOES precipitation index. J. Appl. Meteor. 38: 569 - 579.

MTTM

Megha-Tropiques Technical Memorandum

Laboratoire de Météorologie Dynamique (LMD / IPSL)

Ecole Polytechnique

F-91128 Palaiseau

France

Sophie.Bouffies-Cloche@ipsl.jussieu.fr

http://meghatropiques.ipsl.polytechnique.fr/available-documents/mttm/index.html